VOL. 17, NO. 3, FEBRUARY 2022 ISSN 1819-6608
ARPN Journal of Engineering and Applied Sciences

www.arpnjournals.com

LATERAL TORSIONAL BUCKLING OF BEAMS BENT ABOUT THEIR SINGLE AXIS OF SYMMETRY BY FEM WITH LINEAR ELEMENTS

Nazzal S. Armouti
Department of Civil Engineering, the University of Jordan, Amman, Jordan
E-Mail: armouti@ju.edu.jo

ABSTRACT

As the exact solution of lateral torsional buckling of elastic prismatic beams is practically limited to the simple case of simply supported beam under equal end moments, other loading conditions and boundary conditions require more practical solutions of the problem. Finite element analysis using linear elements (beam elements) is formulated for lateral torsional buckling of beams bent about their symmetric major axis. Finite element development shows that the characteristic equation is function of the square of the critical moment which indicates that for symmetric beams, the critical moment is independent of the sign of the applied moment. This development indicates that lateral torsional buckling of beams is analogous to the frequency analysis of beams which is also independent of the vibration direction as the frequency also appears squared in the characteristic equations. Using the classical polynomial shape functions for beams, finite element method proves to be extremely accurate, efficient, and simple to apply for analysis of lateral torsional buckling of beams. Comparison with code approximate methods, finite element method, FEM, proves to offer more uniform factor of safety (reliability index) across various cases of loading schemes and boundary conditions.

Keywords: finite element method, lateral torsional buckling, symmetric beams.

INTRODUCTION

Lateral torsional buckling of beams is one of the cumbersome problems that faces engineers. In general, lateral torsional buckling can be classified into two categories, first, beams with sections symmetric about their major axis and at the same time bent about this major axis, and second, asymmetric beams or monosymmetic beams about their minor axis and bent about their major axis; the other axis of symmetry (Timoshenko, 1961, Galambus, 1968).

Many analytical and experimental studies have been conducted to tackle the problem of lateral torsional buckling, LTB. LTB of beams is considered a 3D problem, and is usually treated with 3D finite element method, FEM, using shell elements. For examples, 3D shell elements are used to study the collapse of LTB of stepped I-sections (Kweenisky *et al*. 2020), 3D shell elements are used to study LTB of T-beams with opening (Ahmad, 2021), 3D elements are used to study LTB of eccentrically loaded Channel (Dahmani *et al*. 2015), and 3D elements are used to study LTB of a frame (Sabat, 2009). In addition, experimental and numerical analysis are used to study LTB of cantilevered I-section (Demirhan et al. 2020), experimental and numerical analysis are used to study LTB of steel beams under impact loading (Zhang *et al.* 2018), and experiments are used to study LTB of partially restrained high strength steel beams (Wang et al. 2021).

In this paper, FEM with linear elements will be developed as it offers accuracy, efficiency, and simplicity of application over the cumbersome modeling of shell elements.

The exact solution of lateral torsional buckling problem exists for the simple case of simply supported beam under equal end moment. Other support conditions and loading schemes are treated mainly by empirical method. Over the years, the American Institute of Steel Construction, AISC, (AISC, 2017) provides empirical equations with some coefficient of moment to treat such cases. Recent issues of AISC steel manual dropped such crude approximation for asymmetric beams and called for more practical and realistic methods to treat the general case of lateral torsional buckling of beams. Within this context, finite element method offers an attractive and practical solution to this problem.

Due to the length of treatment of both categories, symmetric and asymmetric, this paper will address the first class of beams, i.e. symmetric beams, leaving the second class to future papers. The differential equation of lateral torsional buckling for symmetric beams is obtained by second order analysis (Galambus, 1968, Chen and Lui, 1987), which is given in the following form

$$EC_w\phi^{iv} - GJ\phi'' - \frac{M_o^2}{EI_y}\phi = 0$$

where

E	= Young modulus.
G	= Shear modulus.
C_w	= warping constant, also known as warping moment of inertia, I_ω, (m^6).
J	= Saint Venant torsional constant, (m^4).
I_y	= moment of inertial of the cross section about its weak axis, y, (m^4) as shown in Figure-1.
M_o	= externally applied moment as shown in Figure-1.
ϕ	= twisting angle of the cross section about z-axis as shown in Figure-1, (rad)
ϕ'', ϕ^{iv}	= second and four derivative of, ϕ, with respect to the axis, z.

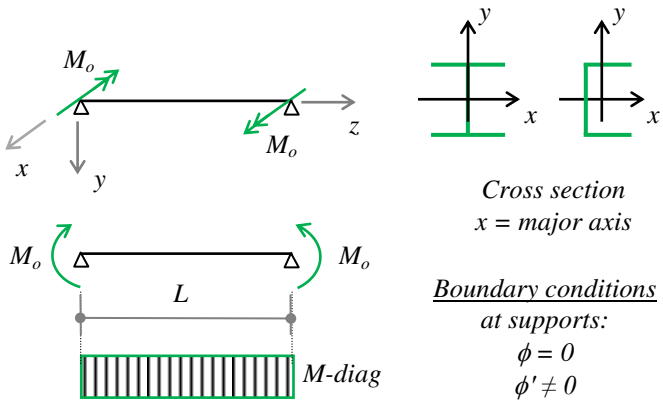

Figure-1. Simply supported beam under equal end moments, free to warp, and braced against rotation at supports.

Within this context, bracing conditions will be identified as follows:

* Simple brace: a brace that provides restriction of the rotation angle, but permits warping at the section under consideration, i.e. $\phi = 0$, $\phi' \neq 0$.
* Fixed brace: a brace that provides restriction for both rotation and warping of the section under consideration, i.e. $\phi = 0$, $\phi' = 0$.

The exact solution of the case of simply supported beam under equal end moments, bent about their symmetric major axis, free to warp, and laterally braced against rotation at the supports, as shown in Figure-1, is given by the following form (Galambus, 1968)

$$M_{ocr} = \pm \frac{\pi}{L}\sqrt{EI_y\, GJ + (\frac{\pi}{L})^2\, EI_y\, EC_w}$$

It is worth mentioning that this case is considered a reference case for lateral torsional buckling in beams analogous to Euler buckling load in columns. The general solution to lateral torsional buckling considers this basic moment, M_{ocr}, as part of the solution as will be presented later. Note also that the above expression includes two equal solution which indicates that the critical moment is independent of the direction of the moment, which is not the case in asymmetric cross sections.

FINITE ELEMENT FORMULATION

To obtain the finite element solution of this problem, Galerkin method of finite element formulation, which operates directly on the differential equation, offers an attractive approach to accomplish this task. Quick review of Galerkin Method (Huebner and Thornton, 1981) reveals that an approximate function of the solution (shape functions) can be assumed, and then minimization of the error by weighted residuals yields the required results. It is well documented that the weighted residuals in Galerkin method are taken as the shape functions themselves.

Accordingly, for the differential equation presented earlier, the twisting angle, $\phi(z)$, may be approximated as, $\bar{\phi}(z)$, which can be expressed in terms of shape functions as follows:

$$\bar{\phi}(z) = \sum_j \psi_j(z)\, \phi_j$$

where

$\bar{\phi}(z)$ = approximate continuous function of field twisting angle.

$\psi_j(z)$ = continuous shape function of field twisting angle, ϕ.

ϕ_j = nodal twisting angle.

If the function, $f(z)$, is defined such as

$$f(z) = EC_w\phi^{iv} - GJ\,\phi'' - \frac{M_o^2}{EI_y}\phi = 0$$

And if the approximate function, $\bar{\phi}(z)$, is used instead of the exact function, $\phi(z)$, then, $f(z)$, becomes approximate function, $\bar{f}(z)$, which does not vanish but yields a residual value, or an error due to the approximation, i.e.

$$\bar{f}(z) = EC_w\bar{\phi}^{iv} - GJ\,\bar{\phi}'' - \frac{M_o^2}{EI_y}\bar{\phi} \neq 0 = \text{residual value}$$

Consequently, there will be an error in the solution equals to the difference between the approximate and exact solution, i.e.

$$\text{error} = \bar{f}(z) - f(z) = \bar{f}(z) - 0 = \bar{f}(z)$$

The weighted residuals method states that the summation of the error components multiplied by their weights is set to zero. Galerkin contribution to this method was to consider the weights to be the shape functions

themselves, hence, the integrated weighted residuals become

$$\int \text{error} \cdot \text{weight} \cdot dz = 0$$

$$\text{or, } \int \left(EC_w \bar{\phi}^{iv} - GJ \bar{\phi}'' - \frac{M_o^2}{EI_y} \bar{\phi} \right) \cdot \psi_i \, dz = 0$$

Substitution of $\bar{\phi}(z) = \sum_j \psi_j(z) \phi_j$

$$\text{then, } \sum_j \int \left(EC_w \psi_j^{iv} \phi_j - GJ \psi_j'' \phi_j - \frac{M_o^2}{EI_y} \psi_j \phi_j \right) \cdot \psi_i \, dz = 0$$

$$\text{or, } \sum_j \int \left(EC_w \psi_j^{iv} \psi_i \phi_j - GJ \psi_j'' \psi_i \phi_j - \frac{M_o^2}{EI_y} \psi_j \psi_i \phi_j \right) \cdot dz = 0$$

By integration by parts, the above integrals can be converted into symmetric integrals which yields the following expression

$$\sum_j \int \left(EC_w \psi_i'' \psi_j'' \phi_j + GJ \psi_i' \psi_j' \phi_j - \frac{M_o^2}{EI_y} \psi_i \psi_j \phi_j \right) \cdot dz = 0 \quad \ldots \; i = 1, 2, 3, 4$$

Note that the highest derivative in the integrals above is a second derivative, and hence, the shape functions must maintain continuity at the nodes up to the first derivative, i.e. ϕ'. Consequently, the beam needs four Degrees of Freedoms (DOFs) to satisfy this continuity requirements, namely, twisting angle and its first derivative at each node of the beam. Note also that these four DOFs require four shape functions. For beams, the popular four polynomial shape function shown in Figure-2, are ideal for this development.

$$\psi_1 = +1 - 3\left(\frac{x}{L}\right)^2 + 2\left(\frac{x}{L}\right)^3$$

$$\psi_2 = +x\left(1 - \frac{x}{L}\right)^2$$

$$\psi_3 = +3\left(\frac{x}{L}\right)^2 - 2\left(\frac{x}{L}\right)^3$$

$$\psi_4 = -\left(\frac{x^2}{L}\right)\left(1 - \frac{x}{L}\right)$$

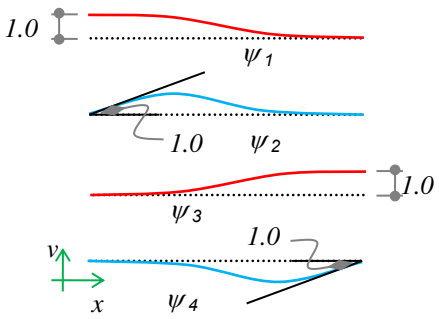

Figure-2. Popular polynomial shape functions used for beam formulation.

The integration of the expression given above yields the corresponding 4x4 element matrices which may be identified and given within this context as follows:

1. Element warping stiffness matrix, $[C_{we}]$, where $C_{we\,ij} = \int EC_w \psi_i'' \psi_j'' \, dz$

$$\text{or, } [C_{we}] = \frac{EC_w}{L^3} \begin{bmatrix} 12 & 6L & -12 & 6L \\ 6L & 4L^2 & -6L & 2L^2 \\ -12 & -6L & 12 & -6L \\ 6L & 2L^2 & -6L & 4L^2 \end{bmatrix}$$

2. Element Saint Venant stiffness matrix, $[J_e]$, where $J_{e\,ij} = \int GJ \psi_i' \psi_j' \, dz$

$$\text{or, } [J_e] = \frac{GJ}{30L} \begin{bmatrix} 36 & 3L & -36 & 3L \\ 3L & 4L^2 & -3L & -L^2 \\ -36 & -3L & 36 & -3L \\ 3L & -L^2 & -3L & 4L^2 \end{bmatrix}$$

3. Element lateral stiffness matrix, $[I_{ye}]$, where I_{ye}

$$_{ij} = \int \frac{1}{EI_y} \psi_i \psi_j \, dz$$

$$\text{or, } [I_{ye}] = \frac{L}{420\,EI_y} \begin{bmatrix} 156 & 22L & 54 & -13L \\ 22L & 4L^2 & 13L & -3L^2 \\ 54 & 13L & 156 & -22L \\ -13L & -3L^2 & -22L & 4L^2 \end{bmatrix}$$

As pointed out earlier, continuity requirements results in four nodal DOFs with 2DOFs at each end. Figure-3 shows the resulting arrangement of these local (element) DOFs as related to the above element matrices. In this paper, the rotation angle will be represented by a curve with single arrow head whereas the twisting curvature is represented by a curve with double arrow heads as shown in Figure-3. Using the vector {U} to represent the local (element) DOFs, the {U} vector appears as follows:

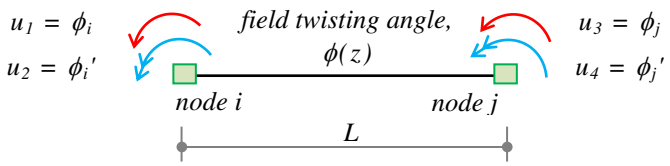

Figure-3. Definition of element Degrees of Freedom of beams in terms of twisting angle, ϕ

$$\{U\} = \begin{Bmatrix} u_1 \\ u_2 \\ u_3 \\ u_4 \end{Bmatrix}, \text{ which is correspondent to,}$$

$$\{\phi\}_{element} = \begin{Bmatrix} \phi_i \\ \phi_i' \\ \phi_j \\ \phi_j' \end{Bmatrix}, \text{ as shown in Figure-3.}$$

Accordingly, the element local matrices take the form

$[C_{we}]\{U\}, \quad [J_e]\{U\}, \quad [I_{ye}]\{U\}$

Recall that curvature is defined as the rate of change of rotation with respect to length, and hence, ϕ', may be viewed as a twisting curvature which is resulting from the effect of warping integral in this case. Note that this twisting curvature appears in this formulation as a new and additional DOF to the beam which becomes the so-called the seventh DOF of the beam modeling including the effect of warping in the section.

In view of the above, and after constructing the counterpart global matrices by the standard assembly process, the finite element formulation may be symbolically presented in matrix form. Using the vector {D} to represent the global DOFs, and for a number of DOFs equals to, N, the final matrix formulation is given as follows

$$[C_w]\{D\} + [J]\{D\} - M_o^2 [I_y]\{D\} = \{0\}$$
$$\text{or, } \{ [C_w] + [J] - M_o^2 [I_y] \}\{D\} = \{0\}$$
$$\text{or, } \{ [[C_w] + [J]] - M_o^2 [I_y] \}\{D\} = \{0\}$$

where

$[C_w]$ = Global warping stiffness matrix size NxN.
$[J]$ = Global Saint Venant stiffness matrix size NxN.
$[I_y]$ = Global lateral stiffness matrix size NxN.
M_o = Lateral torsional moments with numbers equal to N.
$\{D\}$ = Global nodal vector size Nx1 as defined previously.
$= \{ d_1\ d_2\ d_3 \ldots d_N \}^T$

Recall that a standard eigenvalue problem for the two matrices, [A] and [B], is given in the following form

$$\{ [A] - \lambda [B] \}\{\phi\} = \{0\}$$

where, λ and ϕ, are the resulting eigenvalues and eigenvectors.

Therefore, the above lateral torsional buckling matrices represent a set of homogeneous linear algebraic equations with a size equals to, N, and hence represent the characteristic equation of the lateral torsional buckling moments. The solution is a standard eigenvalue problem of the square of the lateral torsional buckling moment which yields an, N, lateral torsional buckling moments and an, N, corresponding mode shapes.

The above development is implemented by programming and coding these procedures using Visual Basic language for application as will be illustrated in the next sections.

FINITE ELEMENT APPLICATION AND VERIFICATION

The application procedures and verification of this method will be demonstrated by considering the beam shown in Figure-4. Using middle line dimensions, the relevant section properties are calculated as shown in Table-1.

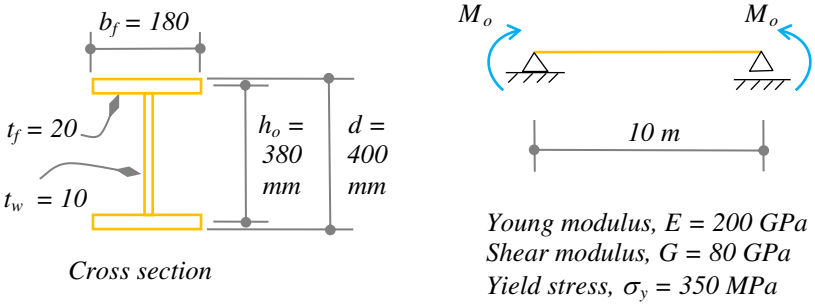

Figure-4. Beam layout and boundary conditions, simple supports with simple braces, i.e. $\phi = 0$, $\phi' \neq 0$

Table-1. Section property calculations.

	Equation expression	Arithmetic detail	Section property value	Stiffness value
Warping constant, C_w	$I_F \frac{h_o^2}{2}$	$\left(\frac{20(180)^3}{12}\right)\left(\frac{380^2}{2}\right)$	$C_w = 701.784 \times 10^9$ mm^6	$EC_w = 140.3568$ kN.m^4
Torsional Constant, J	$\sum \frac{b\,t^3}{3}$	$\left(\frac{180(20)^3}{3}\right)(2)+\left(\frac{360(10)^3}{3}\right)$	$J = 1.08 \times 10^6$ mm^4	$GJ = 86.4$ kN.m^2
Lateral moment of inertia, I_y	$\frac{t_f\, b_f^3}{12}(2)$	$\left(\frac{20(180)^3}{12}\right)(2)$	$I_y = 19.44 \times 10^6$ mm^4	$EI_y = 3{,}888$ kN.m^2

This beam is simply supported, simply braced, and subjected to equal end moments which has an exact solution as presented in the introduction, therefore, the exact lateral torsional moment, M_{ocr}, is given as follows:

$$M_{ocr} = \pm \frac{\pi}{L}\sqrt{EI_y\, GJ + \left(\frac{\pi}{L}\right)^2 EI_y\, EC_w}$$

$$M_{ocr} = \pm \frac{\pi}{10}\sqrt{3{,}888\,(86.4) + \left(\frac{\pi}{10}\right)^2 (3{,}888)\,(140.3568)}$$

$= 196.138$ kN.m

The FEM solution is obtained by standard procedures. In this section, demonstration of the procedures will be presented using two identical elements as shown in Figure-5. Since the supports provide simple brace, i.e. $\phi = 0$, $\phi' \neq 0$, the beam will have four global DOFs, namely, two twisting curvatures at the supports, i.e. at Nodes 1 and 3, and one rotation, one twisting curvature at midspan, i.e. at Node 2 as shown in Figure-5.

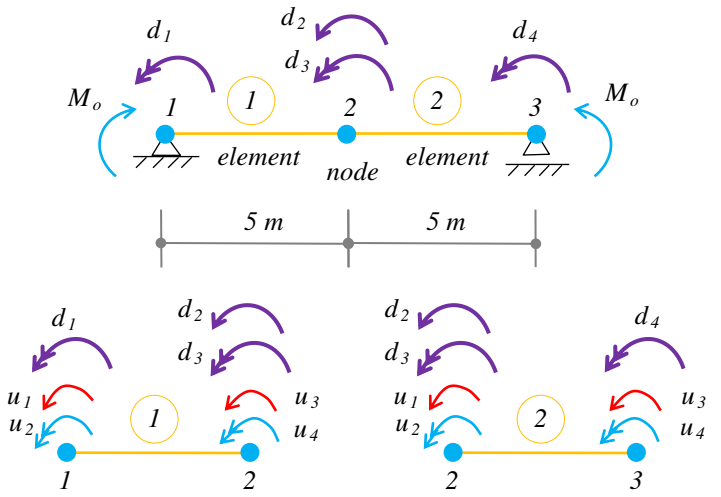

Figure-5. Beam discretization into two equal elements.

Element Matrices

Note that since the two elements are identical, the element matrices will be the same for both of them. Using (kN, m) units, the matrices are calculated as follows

$$[C_{we1}] = [C_{we2}] = [C_{we}] = \frac{EC_w}{L^3}\begin{bmatrix} 12 & 6L & -12 & 6L \\ 6L & 4L^2 & -6L & 2L^2 \\ -12 & -6L & 12 & -6L \\ 6L & 2L^2 & -6L & 4L^2 \end{bmatrix} =$$

$$\begin{bmatrix} 13.474 & 33.686 & -13.474 & 33.686 \\ 33.686 & 112.285 & -33.686 & 56.143 \\ -13.474 & -33.686 & 13.474 & -33.686 \\ 33.686 & 56.143 & -33.686 & 112.285 \end{bmatrix}$$

$$[J_{e1}] = [J_{e2}] = [J_e] = \frac{GJ}{30L}\begin{bmatrix} 36 & 3L & -36 & 3L \\ 3L & 4L^2 & -3L & -L^2 \\ -36 & -3L & 36 & -3L \\ 3L & -L^2 & -3L & 4L^2 \end{bmatrix} =$$

$$\begin{bmatrix} 20.736 & 8.640 & -20.736 & 8.640 \\ 8.640 & 57.600 & -8.640 & -14.400 \\ -20.736 & -8.640 & 20.736 & -8.640 \\ 8.640 & -14.400 & -8.640 & 57.600 \end{bmatrix}$$

$$[I_{ye1}] = [Y_{ye2}] =$$

$$[I_{ye}] = \frac{L}{420\,EI_y}\begin{bmatrix} 156 & 22L & 54 & -13L \\ 22L & 4L^2 & 13L & -3L^2 \\ 54 & 13L & 156 & -22L \\ -13L & -3L^2 & -22L & 4L^2 \end{bmatrix} =$$

$$10^{-6}\begin{bmatrix} 478 & 337 & 165 & -199 \\ 337 & 306 & 199 & -230 \\ 165 & 199 & 478 & -337 \\ -199 & -230 & -337 & 306 \end{bmatrix}$$

Assembly of the global matrices, $[K_G]$, in terms of the global 4DOFs, d_1, d_2, d_3, d_4, can be carried out from the element matrices, $[k_e]$, using the following expression (Chen and Lui, 1987)

$[K_G] = \Sigma\,[T]^T\,[k_e]\,[T]$ … summation is carried out over all elements

where, [T], is known as the kinematic (compatibility) matrix which relates the global nodal deformations {D} to element nodal deformations {U}. Accordingly, the [T] matrices for elements, 1 and 2, are constructed as follows

$$[T_1]^T = \begin{array}{c} \\ d_1 \\ d_2 \\ d_3 \\ d_4 \end{array}\begin{array}{c} \begin{array}{cccc} u_1 & u_2 & u_3 & u_4 \end{array} \\ \begin{bmatrix} 0 & 1 & 0 & 0 \\ 0 & 0 & 1 & 0 \\ 0 & 0 & 0 & 1 \\ 0 & 0 & 0 & 0 \end{bmatrix} \end{array}, \quad [T_2]^T = \begin{array}{c} \\ d_1 \\ d_2 \\ d_3 \\ d_4 \end{array}\begin{array}{c} \begin{array}{cccc} u_1 & u_2 & u_3 & u_4 \end{array} \\ \begin{bmatrix} 0 & 0 & 0 & 0 \\ 1 & 0 & 0 & 0 \\ 0 & 1 & 0 & 0 \\ 0 & 0 & 0 & 1 \end{bmatrix} \end{array}$$

Carrying out the above summation leads to

$$[C_w]_{global} = \Sigma\,[T_i]^T\,[C_{we,i}]\,[T_i] =$$

$$\begin{bmatrix} 112.285 & -33.686 & 56.143 & 0 \\ -33.686 & 26.949 & 0 & 33.686 \\ 56.143 & 0 & 224.571 & 56.143 \\ 0 & 33.686 & 56.143 & 112.285 \end{bmatrix}$$

$$[J]_{global} = \Sigma [T_i]^T [J_{,i}] [T_i] = \begin{bmatrix} 57.600 & -8.640 & -14.400 & 0 \\ -8.640 & 41.472 & 0 & 8.640 \\ -14.400 & 0 & 115.200 & -14.400 \\ 0 & 8.640 & -14.400 & 57.600 \end{bmatrix}$$

$$[I_y]_{global} = \Sigma [T_i]^T [I_{y,i}] [T_i] = 10^{-6} \begin{bmatrix} 306.192 & 199.025 & -229.644 & 0 \\ 199.025 & 955.320 & 0 & -199.025 \\ -229.644 & 0 & 612.385 & -229.644 \\ 0 & -199.025 & -229.644 & 306.192 \end{bmatrix}$$

Characteristic equation:

$$\{ [[C_w] + [J]] - M_o^{\,2} [I_y] \} \{D\} = \{0\}$$

$$\left(\begin{bmatrix} 169.885 & -42.326 & 41.743 & 0 \\ -42.326 & 68.421 & 0 & 42.326 \\ 41.743 & 0 & 339.771 & 41.743 \\ 0 & 42.326 & 41.743 & 169.885 \end{bmatrix} - M_o^{\,2} \right) \left(10^{-6} \right) \begin{bmatrix} 306.192 & 199.025 & -229.644 & 0 \\ 199.025 & 955.320 & 0 & -199.025 \\ -229.644 & 0 & 612.385 & -229.644 \\ 0 & -199.025 & -229.644 & 306.192 \end{bmatrix} \begin{Bmatrix} d_1 \\ d_2 \\ d_3 \\ d_4 \end{Bmatrix} = \begin{Bmatrix} 0 \\ 0 \\ 0 \\ 0 \end{Bmatrix}$$

Standard solution of the above eigenvalue equation yields four moments, $\{M_o\}$, and four mode shapes, $[\phi]$, as follows

$$\{M_o\} = \begin{Bmatrix} 196.274 \\ 489 \\ 989 \\ 1{,}663 \end{Bmatrix}, \quad [\ \phi\ ] = \left[\phi_1 \vdots \phi_2 \vdots \phi_3 \vdots \phi_4 \right] = \left[\begin{array}{c:c:c:c} 1 & 1 & 1 & 1 \\ 3.162 & 0 & -0.547 & 0 \\ 0 & -1 & 0 & 1 \\ -1 & 1 & -1 & 1 \end{array} \right]$$

Graphical presentation of the mode shapes are also shown in Figure-6. The critical lateral torsional buckling moment is, of course, the smallest of the four moments which is given as follows:

M_{ocr} = 196.274 kN.m … vs … exact = 196.138 kN.m

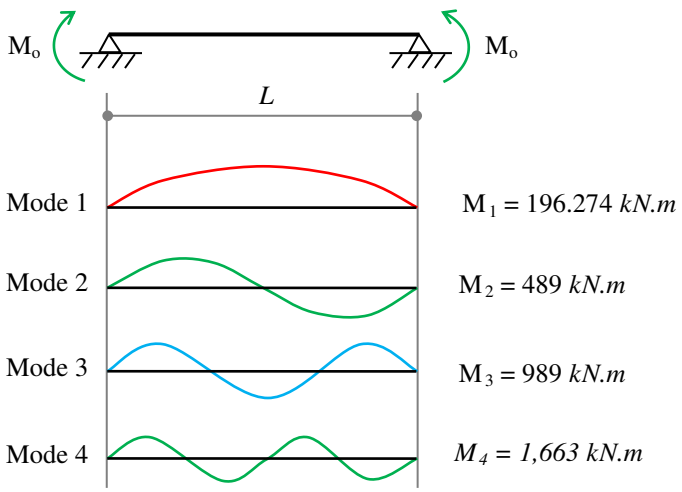

Figure-6. Buckling moments and their mode shapes.

As well-known and documented, the accuracy of the FEM solution depends on the size of the mesh (number of elements) in this case. In order to examine the effect of the mesh size on the accuracy of this solution, the above procedures are repeated for, 1, 2, 3, 5, and 10 elements. The results are summarized in Table-2.

Table-2. Critical lateral torsional buckling moment for various FEM mesh sizes.

	Exact solution	Number of elements				
		1	2	3	5	10
Critical moment, M_{ocr} (kN.m)	196.138	200.352	196.274	196.163	196.141	196.138
% error	0 %	2.15 %	0.07 %	0.01 %	0.0015 %	≅ 0 %

Table-2 shows that the accuracy of the solution is excellent and becomes almost exact if, 10, elements are used. It can also be seen that using one element which is considered very crude mesh, the error is still around 2%. For all practical purposes, it can be seen that two elements are more than enough to get very accurate results (.07% error). However, in the general case where moment gradient or even cross section are not constant but rather varies along the axis of the beam, a number of elements should be selected to capture the effect of such variations in what is known as sensitivity analysis in FEM.

THE GENERAL CASE AND COMPARISON WITH AISC PROVISIONS

AISC treats the general case of lateral torsional buckling by the help of the well-known concept of equivalent moment coefficient, C_b. In this approach, the critical moment of the basic case of simply supported beam under equal end moment, M_{ocr}, is calculated and then multiplied by the coefficient, C_b, to account for the difference in the end moments, and later revised to account for the moment gradient between the bracing points. Accordingly, the critical moment, M_{cr}, is calculated as

$$M_{cr} = C_b M_{ocr}$$

As can be interpreted from the above expression, the coefficient, $C_b = M_{cr} / M_{ocr}$, may be viewed as an indicator for the critical moment in the beam which will be used later for comparison between various cases.

For many years, AISC used Salvadori (Salvadori, 1955) expression for, C_b, which is a function of the values of the end moments at the bracing points without consideration of the moment gradients due to transverse loads. Salvadori expression for, C_b, is given as follows

$$C_b = 1.75 + 1.05\left(\frac{M_A}{M_B}\right)_d + 0.3\left(\frac{M_A}{M_B}\right)_d^2 \leq 2.3$$

where

M_A = smaller of the two end moments at the bracing points.

M_B = larger of the two end moments at the bracing points.

M_A/M_B = is the ratio of end moments taken positive when bent is double curvature.

In the past decade, AISC replaced Salvadodri expression by another empirical expression that takes moment gradient into consideration which was developed by Kirby and Nethercot (Kirby and Nethercot, 1979). ASIC used a slightly modified, and more conservative form of Kirby and Nethercot expression which is given in its modified form as follows:

$$C_b = \frac{12.5\, M_{max}}{2.5\, M_{max} + 3\, M_A + 4\, M_B + 3\, M_C} \leq 3$$

where

M_{max} = absolute maximum moment between bracing points.

M_A = absolute moment at one quarter point between bracing points.

M_B = absolute moment at midpoint between bracing points.

M_C = absolute moment at three quarter point between bracing points.

As is expected, the FEM is a general solution that has no limits of including boundary conditions, cross section variation, and loading conditions in the analysis. As this method is rather accurate, it will be used to examine the accuracy, or the conservatism, embedded in the empirical expressions of the equivalent moment coefficient, C_b, for some popular cases.

For discussion and comparison purposes, eight cases which are broken into three groups will be examined. Group I examines three beams subject to end moments only, Group II examines three beams subject to transverse loads with various boundary conditions, whereas Group III examines two beams with continuous spans.

Group I: Beams Subject to End Moments Only

In this group of beams, which are the origin of the development of, C_b, the internal moment in the beam will be linear and function of the moments at the ends as shown in Figure-7. Figure-7 shows three popular cases with externally applied moments to simply supported beams. The results of buckling moments for these three cases are as shown in Table-3.

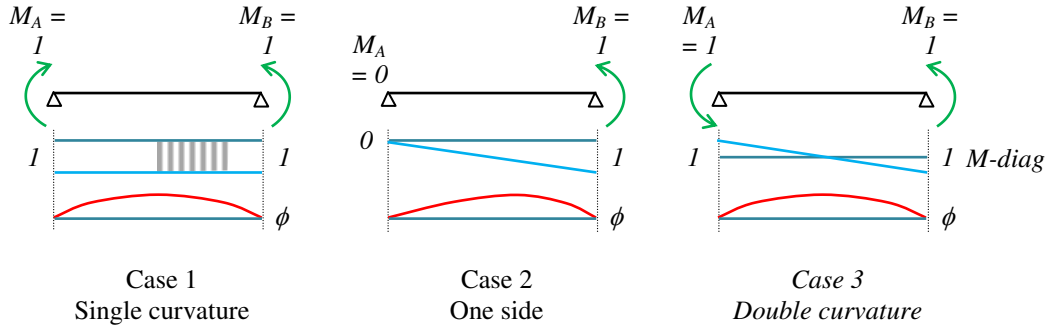

Figure-7. Group I: Beams subject to end moments only
Moment diagrams and mode shapes, ϕ-angle

Table-3. Comparison between empirical expressions and FEM solution Group I: Beams subject to end moments only.

Method of Analysis	Coefficient of Moment, C_b					
	Case 1		Case 2		Case 3	
	C_b	C_b / $C_{b,FEM}$	C_b	C_b / $C_{b,FEM}$	C_b	C_b / $C_{b,FEM}$
Salvadori	1	1	1.75	0.97	2.30	0.87
Modified Kirby and Nethercot (AISC)	1	1	1.67	0.95	2.27	0.86
FEM	1	1	1.80	1	2.64	1

It can be noted from Table-3 that even though Salvadori, and Modified Kirby and Nethercot expressions are conservative, they do not offer consistent level of reliability among the different cases. For example, Case 3 shows larger conservative levels of the buckling moment than Cases 1 and 2.

Group II: Beams Subject to Transverse Loads

Figure-8 shows three cases with externally applied transverse loading with or without externally applied end moments for various boundary conditions. The results of buckling moments for these three cases are shown in Table-4.

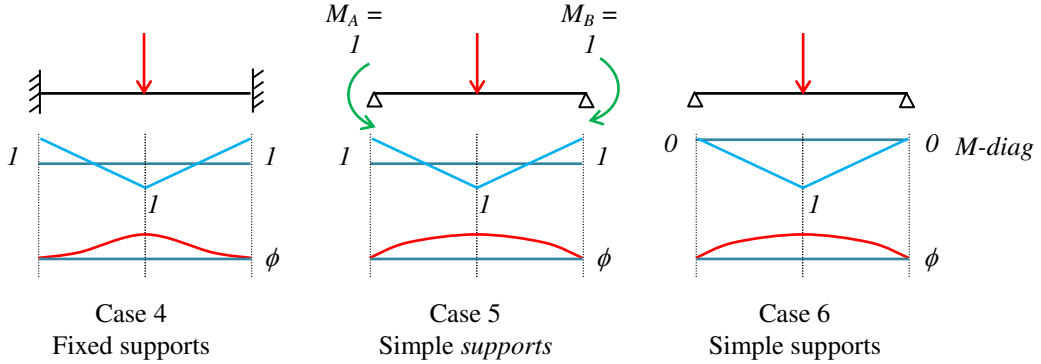

Figure-8. Group II: Beams subject to transverse loading
Moment diagrams and mode shapes, ϕ-angle

Table-4. Comparison between empirical expressions and FEM solution
Group II: Beams subject to transverse loads.

Method of Analysis	Coefficient of Moment, C_b					
	Case 4		Case 5		Case 6	
	C_b	C_b / $C_{b,FEM}$	C_b	C_b / $C_{b,FEM}$	C_b	C_b / $C_{b,FEM}$
Salvadori	1	0.45	1	0.57	1	0.73
Modified Kirby and Nethercot (AISC)	1.92	0.87	1.92	1.10	1.32	0.96
FEM	2.20	1	1.75	1	1.37	1

Table-4 shows that both Salvadori, and Modified Kirby and Nethercot expressions do not recognize warping DOF, ϕ', which affects the buckling moments. Figure-8 shows that Case 4, which has fixed supports (restricted warping), and Case 5, which has simple support (unrestricted warping) have identical moment diagram. Consequently, Salvadori, and Modified Kirby and Nethercot expressions yield the same value of, C_b, for Case 4 and for Case 5. However, FEM results indicates that restricting warping, i.e. ϕ' = 0, strengthens the beam, as would be expected, and increases the buckling moment even for the same moment diagram. Table-4 indicates that FEM yields higher buckling moment for Case 4 than for Case 5 due to their different boundary conditions even with identical moment diagram.

Group III: Continuous Beams

Figure-9 shows two cases with continuous beams subject to transvers loading, Case 7 take warping constant into consideration whereas Case 8 ignores warping constant in the analysis. The results of buckling moments for these two cases are shown in Table-5.

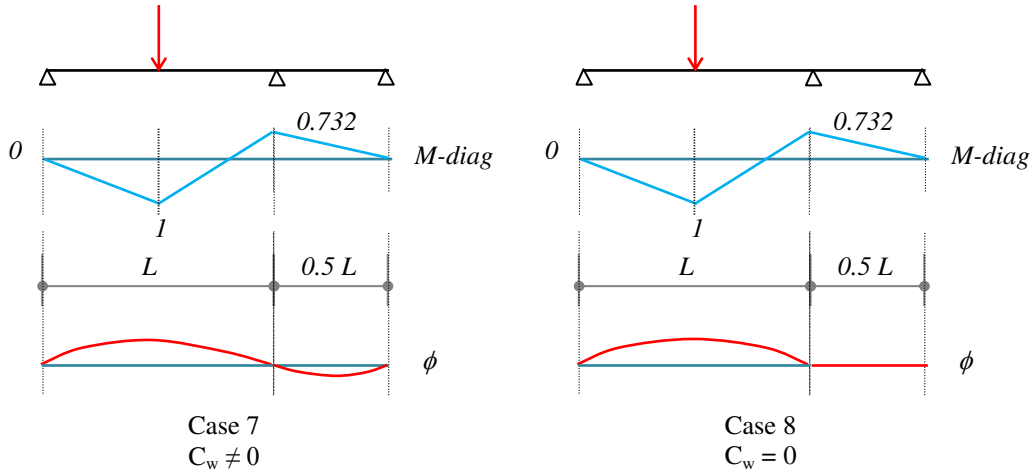

Figure-9. Group III: Continuous beams
Moment diagrams and mode shapes, ϕ-angle

Table-5. Comparison between empirical expressions and FEM solution Group III: Continuous beams.

Method of Analysis	Coefficient of Moment, C_b							
	Case 7 ($C_w \neq 0$)				Case 8 ($C_w = 0$)			
	Right span ignored		Continuous beam		Right span ignored		Continuous beam	
	C_b	C_b / $C_{b,FEM}$	C_b	C_b / $C_{b,FEM}$	C_b	C_b / $C_{b,FEM}$	C_b	C_b / $C_{b,FEM}$
Salvadori	1.75	1.17	1.75	1.11	1.75	1.27	1.75	1.27
Modified Kirby and Nethercot (AISC)	1.49	0.99	1.49	0.94	1.49	1.08	1.49	1.08
FEM	1.50	1	1.58	1	1.37	1	1.37	1

It can be observed from Table-5 that the values of, C_b, obtained from both Salvadori (C_b = 1.75) and Modified Kirby and Nethercot (C_b = 1.49) expressions are the same regardless of the consideration of warping or continuity of the beam (multiple spans). These results indicate again that these expressions do not recognize the warping or continuity of the beam. These limitations can clearly be overcome and inherently covered by FEM formulation.

CONCLUSIONS

As recent versions of some reputable steel codes reveal that they are uneasy with their current procedures of treatment of lateral torsional buckling of beams, and hence call for more practical and realistic methods in treatment of this problem, it has been shown that Finite Element Method offers the ideal solution for this problem. In this paper, FEM with linear elements (beam elements) is developed which offers simplicity, efficiency, and accuracy to evaluate the lateral torsional buckling moments for various cases of various loading schemes and boundary conditions.

This approach offers its simplicity over using three dimensional shell elements to deal with this problem which is apparently a cumbersome task. In this method, the modeling of beams as linear elements will be simple, in addition, it allows the direct and simple application of moments at different locations along the axis of the beam as required.

The developed FEM procedures are then used to examine various cases of loading schemes and boundary conditions which shows that the currently used code procedures in some steel codes do not always offer conservative solution nor offers consistent factor of safety (reliability index). Therefore, using FEM overcomes this inconsistency by offering a more uniform reliability level among the various cases of loading schemes and boundary conditions.

It is also shown that the current code methods of treatment and the expressions used accordingly do not recognize many situations of boundary conditions, continuity of the beam, geometry, and warping properties. FEM can further overcome these inconsistency in the analysis and offer natural incorporation of these variations along the axis of the beam.

It is worth reminding the reader that this paper treats symmetric beams only, which are characterized by having their shear center lying on the major axis of bending. The general case will be totally different which is intended to be treated separately in the near future.

REFERENCES

Ahmad N. Z. 2021. Numerical parametric study on lateral torsional buckling of T-shaped beams containing openings. Journal of Xi'an University of Architecture & Technology, Xi'an, China. VIII (1): 570-585.

AISC. 2017. Specification for Structural Steel Buildings. American Institute of Steel Construction, Chicago, IL 606017.

Chen W. F. and Lui E. M. 1987. Structural Stability, Theory and Implementation. Elsevier, New York.

Dahmani L., Drizi S., Djemai M., Boudjemia A. and Mechiche M. O. 2015. Lateral Torsional Buckling of an Eccentrically Loaded Channel Section Beam. International Journal of Civil and Environmental Engineering. 9(6): 689-692.

Demirhan A. L., Eroglu H. E., Mutlu E. O., Yilmaz T. and Anil O. 2020. Experimental and Numerical Evaluation of Inelastic Lateral-torsional Buckling of I-section Cantilevers. Journal of Constructional Steel Research, Elsevier. Vol. 168 (105991).

Galambus T. V. 1968. Structural Members and Frames. Prentice-Hall, Englewood, Cliffs, New Jersey.

Huebner K. H. and Thornton E. A. 1981. The Finite Element Method for Engineers. 2nd ed., John Wiley & Sons, New York.

Kirby P. A. and Nethercot D. A. 1979. Design for Structural Stability. Constrado Monographs, Granada Publishing, UK.

Kweenisky K. T., Pratiwi N. and Wijaya P. K. 2020. Collapse Analysis of the Lateral-torsional Buckling of I-shaped Stepped Steel Beams. Journal of Civil Engineering Forum. 6(3): 295-308.

Sabat A. K. 2009. Lateral-torsional Buckling analysis of steel frames with corrugated webs. Masters thesis, Dept. of Civil Engineering, Chalmers University of Technology, Goteborg, Sweden.

Salvaori M. G. 1955. Lateral Buckling of I-beams. ASCE Transaction. 120: 1165-1177.

Timoshenko S. P. and Gere J. M. 1961. Theory of elastic stability. McGraw-Hill, New York.

Wang K., Xiao M., Chung K. and Nethercot D. A. 2021. Lateral torsional buckling of partially restrained beams of high strength S690 welded I-sections. Journal of Constructional Steel Research, Elsevier. Vol. 184 (106777).

Zhang W., Liu F. and Xi F. 2018. Lateral Torsional Buckling of Steel beams under Transverse Impact Loading. Shock and Vibration, Hindawi. 2018: 1-15.